

1 **Refined mapping of tree cover at fine-scale using time-series**
2 **Planet-NICFI and Sentinel-1 imagery for Southeast Asia (2016-**
3 **2021)**

4 Feng Yang^a, Zhenzhong Zeng^{a, *}

5 ^a School of Environmental Science and Engineering, Southern University of Science and Technology,
6 Shenzhen 518055, China

7

8

9 * Correspondence to: zengzz@sustech.edu.cn (Zhenzhong Zeng)

10 Mailing Address:

11 College of Engineering N808

12 Southern University of Science and Technology

13 Shenzhen, China

14

15

16

17 The manuscript for *Earth System Science Data*

18 July 31, 2023

19

20 **Abstract:**

21 High-resolution mapping of tree cover is indispensable for effectively addressing tropical forest carbon loss,
22 climate warming, biodiversity conservation, and sustainable development. However, the availability of
23 precise high-resolution tree cover map products remains inadequate due to the inherent limitations of
24 mapping techniques utilizing medium-to-coarse resolution satellite imagery, such as Landsat and Sentinel-2
25 imagery. In this study, we have generated an annual tree cover map product at a resolution of 4.77 m for
26 Southeast Asia (SEA) for the years 2016-2021 by integrating Planet-Norway's International Climate &
27 Forests Initiative (NICFI) imagery and Sentinel-1 Synthetic Aperture Radar data. We have also collected
28 annual tree cover/non-tree cover samples to assess the accuracy of our Planet-NICFI tree cover map product.
29 The results show that our Planet-NICFI tree cover map product during 2016-2021 achieve high accuracy,
30 with an overall accuracy of $\geq 0.867 \pm 0.017$ and a mean F1 score of 0.921, respectively. Furthermore, our tree
31 cover map product exhibits high temporal consistency from 2016 to 2021. Compared to existing map products
32 (FROM-GLC10, ESA WorldCover 2020 and 2021), our tree cover map product exhibits better performance,
33 both statistically and visually. Yet, the imagery obtained from Planet-NICFI performs less in mapping tree
34 cover in areas with diverse vegetation or complex landscapes due to insufficient spectral information.
35 Nevertheless, we highlight the capability of Planet-NICFI datasets in providing quick and fine-scale tree
36 cover mapping to a large extent. The consistent characterization of tree cover dynamics in SEA's tropical
37 forests can be further applied in various disciplines. Our data from 2016 to 2021 at a 4.77 m resolution are
38 publicly available at <https://cstr.cn/31253.11.sciencedb.07173> (Yang and Zeng, 2023).

39

40 **1 Introduction**

41 Forests and tree-based systems outside forests play a crucial role in land-based carbon emissions or removals,

42 making them essential for supporting and monitoring the implementation of the Reducing Emissions from
43 Deforestation and Forest Degradation (REDD+) and other land-based activities under the Paris Agreement
44 (Skea et al., 2022; CoP26, 2021; FAO, 2020). However, current forest cover map products exhibit significant
45 errors in accurately estimating forest area and change, particularly in areas such as trees outside forests and
46 forest edge landscapes (Mugabowindekwe et al., 2023; Reiner et al., 2022; Brandt et al., 2020). As a result,
47 there is a growing demand for timely, high-quality, and high-resolution tree cover products to accurately
48 capture the dynamics and changes in tree cover.

49

50 Many tree cover map products have been developed at medium-to-coarse resolutions (10-500 m), such as
51 Finer Resolution Observation and Monitoring of Global Land Cover 10 m (FROM-GLC10; Gong et al.,
52 2019), Environmental Systems Research Institute (ESRI) Land Cover (2017-2021) (Karra et al., 2021),
53 European Space Agency (ESA) WorldCover 2020 and 2021 (Zanaga et al., 2022; Zanaga et al., 2021), GFC
54 (Hansen et al., 2013), Globeland30 (Chen et al., 2015), Copernicus Global Land Service (CGLS) Land Cover
55 (Buchhorn et al., 2020), ESA Climate Change Initiative (CCI) (ESA, 2017) and the National Aeronautics and
56 Space Administration (NASA) MCD12Q1 (Friedl and Sulla-Menashe, 2019). However, accurate high-
57 resolution tree cover map products at continental-to-global scales are still lacking due to mapping through
58 medium-to-coarse resolution imagery (Zanaga et al., 2021; Hansen et al., 2010). Consequently, some
59 uncertainties occur in acquiring global tree inventories and monitoring forest disturbances (deforestation and
60 forest degradation). This is mainly due to isolated trees or long narrow forest cover removal (Reiner et al.,
61 2022; Wagner et al., 2022; Sexton et al., 2016; Hammer et al., 2014; Hsieh et al., 2001).

62

63 Only recently have two tree cover map products at <4.77 m from preprints been produced over Africa and

64 the state of Mato Grosso in Brazil using Planet-Norway's International Climate & Forests Initiative (NICFI)
65 imagery based on deep learning (Wagner et al., 2023; Reiner et al., 2022). However, these two maps have
66 only limited temporal or spatial coverage that occurred. Since the early 21st century, agricultural expansion
67 has created a new wave of drastic land use/land cover changes in Southeast Asia (SEA), leading the region
68 to be one of the most deforested regions worldwide (Zeng et al., 2018a; Zeng et al., 2018b; Achard et al.,
69 2014). Average elevations and slopes of forest loss sites have significantly increased in SEA, particularly in
70 the 2010s, geometrically irregular upland land use sites commonly occur (Velasco et al., 2022; Feng et al.,
71 2021). However, existing tree cover map products have underestimated deforestation (25-116%) and upland
72 agricultural expansion rates (9-113%), especially on the topographic boundaries in SEA (Zeng et al., 2018a).
73 Thus, fine-resolution tree cover map products in SEA, with high spatial resolution and longer consistent time
74 series, are urgently needed to accurately monitor tree cover loss and related illegal deforestation. In addition,
75 combining high-resolution optical imagery and Synthetic Aperture Radar (SAR) data (Sentinel-1) to produce
76 large-area tree cover map products is still in its early stage (Zanaga et al., 2022; Karra et al., 2021; Zanaga et
77 al., 2021; Buchhorn et al., 2020; Hansen et al., 2010).

78
79 Concurrently, advances in large-scale cloud computing (e.g., Google Earth Engine, GEE; Gorelick et al.,
80 2017) and available high-resolution satellite imagery (Roy et al., 2021) can facilitate the development of
81 high-resolution and longer time-series tree cover map products at continental-to-global scales. In this paper,
82 we generated state-of-the-art fine-scale open-source tree cover maps for SEA during 2016-2021 using Planet-
83 NICFI imagery, Sentinel-1 SAR data, and the random forest (RF) method from a previous study (Yang et al.,
84 2023). This dataset allows for extensive assessments of forest dynamics change, such as deforestation, forest
85 degradation, and reforestation. In addition, our dataset can monitor trees outside forests and long narrow

86 forest cover removal, thus improving the accuracy of automated continental tree inventories, which helps
87 optimize REDD+ under the Paris Agreement.

88

89 **2 Materials and method**

90 **2.1 Satellite imagery**

91 We utilized Planet-NICFI and Sentinel-1 imagery for the years 2016-2021 to generate a time series tree cover
92 map product for SEA. The Planet-NICFI program provides high-resolution (4.77 m per pixel) optical
93 PlanetScope surface reflectance mosaics specifically designed for the tropics. These mosaics offer accurate
94 and reliable spatial data with minimized effects from atmosphere and sensor characteristics, making them an
95 ideal 'ground truth' representation (Planet Team, 2017). The mosaics cover the best imagery to represent every
96 part of the coverage area during leaf-on periods from June to November based on cloud cover and acutance
97 (image sharpness). The Planet-NICFI imageries consist of four bands: red, green, blue, and near-infrared, and
98 cover a time period from 2015 to 2020 at bi-annual resolution for the archive, and from 2020 to 2023 at
99 monthly resolution for monitoring purposes. We accessed and utilized these products in the GEE platform by
100 authorizing our NICFI account to the GEE account.

101

102 We utilized Sentinel-1 on the GEE platform, specifically the 10 m resolution dual-polarization Ground Range
103 Detected (GRD) scenes (VV + VH). We chose Sentinel-1 SAR imagery to correct cases of overestimation
104 caused by confusion with herbaceous vegetation, or underestimation due to optical satellite observations
105 omitting deciduous or semi-deciduous characteristics (Shimada et al., 2014). The SAR imagery, available
106 every 12 days for a single satellite or 6 days for a dual-satellite constellation from October 2014 to the present,
107 was pre-processed with the Sentinel-1 Toolbox for thermal noise removal, radiometric calibration, and terrain

108 correction.

109

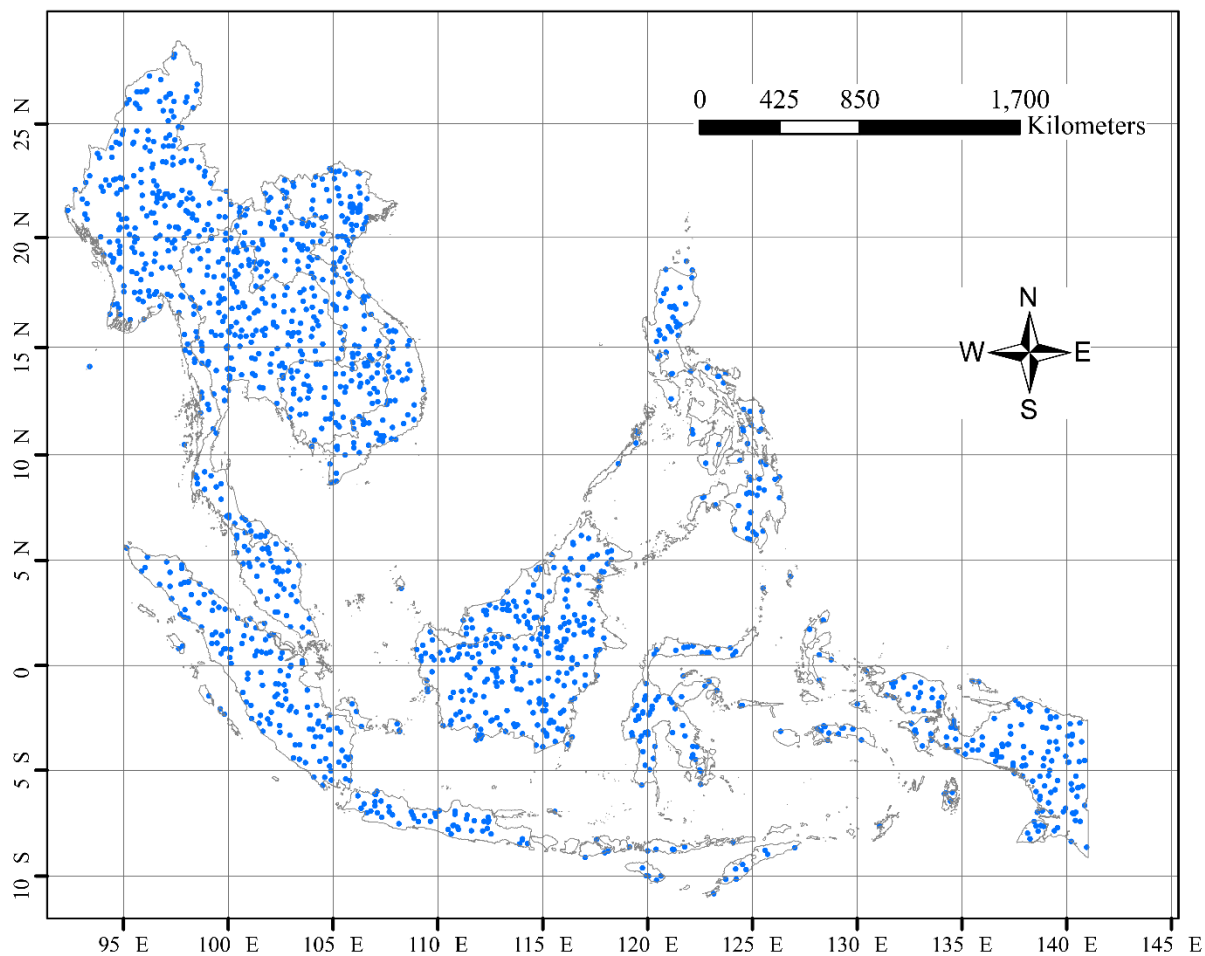
110 **2.2 Validation dataset collection**

111 We collected time series validation datasets to comprehensively assess the tree cover map product during
112 2016-2021, except for 2019 as it has been provided by Yang et al. (2023). Our mapping approach has been
113 comprehensively assessed after being developed in 2019 (Yang et al., 2023). However, despite the
114 advancements in the Land Cover Land Use Change (LCLUC) community, a notable gap remains the absence
115 of publicly available high-resolution (e.g., ≤ 10 m) tree cover/non-tree cover labels. The existing coarse-
116 resolution labels for tree cover/non-tree cover can introduce considerable uncertainties when evaluating high-
117 resolution tree cover maps. As a result, our ability to delve deeper into the accuracy of time-series tree cover
118 map datasets was hindered.

119

120 Following the methodology established by Yang et al. (2023), we undertook a rigorous process to generate a
121 robust validation dataset for our study. Firstly, we randomly generated 1,515 points to ensure a representative
122 sample of collected visual data, as illustrated in Fig. 1. Next, to classify these points as trees or non-trees, we
123 enlisted four human interpreters and employed Planet Explorer within QGIS. Our approach involved visually
124 identifying tree cover/non-tree cover pixels in the true color composite of Planet-NICFI imagery where the
125 points were located. To ensure accuracy, we superimposed the 10 m tree height data, previously developed
126 by Lang et al. (2022), onto the Planet-NICFI imagery. This step ensured that the labels adhered to the specified
127 tree height criteria (i.e., ≥ 5 m). Subsequently, we thoroughly evaluated and refined the labels using Google
128 Earth. To make time series tree cover/non-tree cover labels, we maintained the geographic location of the
129 1,515 points and changed the year of the Planet-NICFI imagery. The resulting labels encompassed data from

130 the years 2016, 2017, 2018, 2020, and 2021. Comprehensive information about the validation dataset can be
 131 found in Table 1.



132
 133 **Figure 1** Spatial distribution of randomly generated 1,515 validation dataset points.

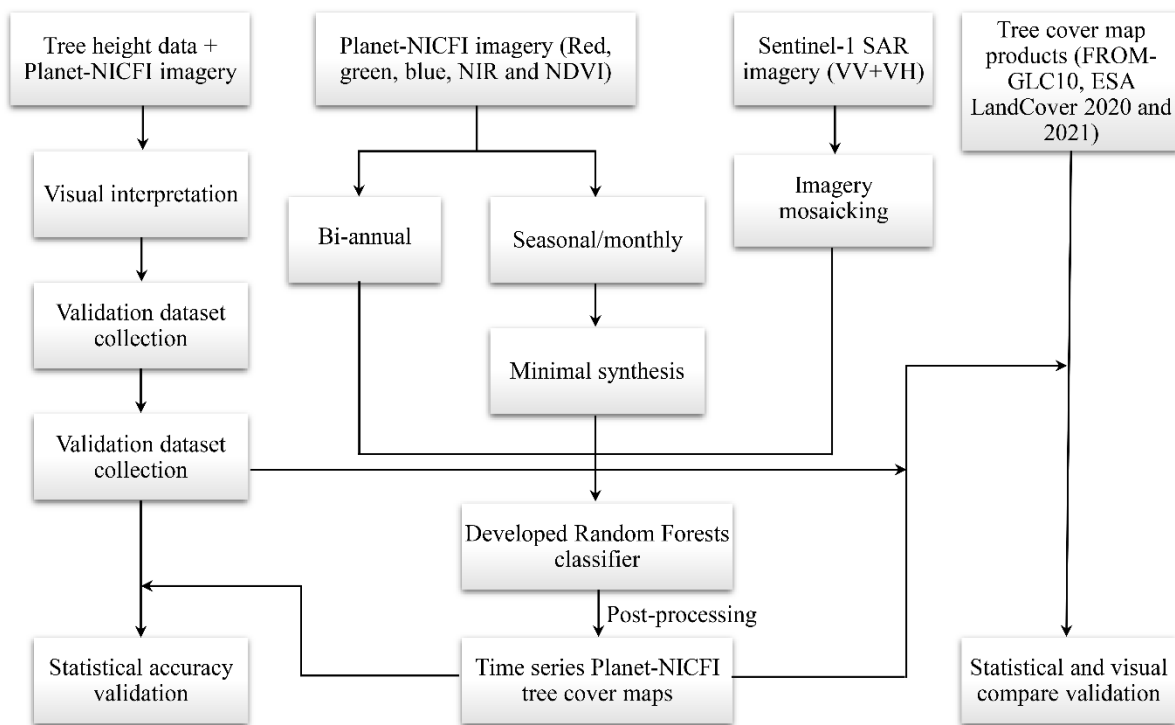
134
 135 **Table 1** Information of the mapped validation dataset for evaluating the generated tree cover map product.

Period	Count of sample points		
	Tree cover	Non-tree cover	Total
2016	1,086	429	1,515
2017	1,026	489	1,515
2018	977	538	1,515
2020	1,093	422	1,515
2021	952	563	1,515

136

137 **2.3 Method**

138 We integrated Planet-NICFI and Sentinel-1 SAR imagery to generate a high-resolution (4.77 m) annual tree
139 cover map product for SEA covering the years 2015-2021. Our framework involved several key steps,
140 including defining mapped objects, preprocessing of imagery, and generation of time-series tree cover map
141 product. The detailed workflow is illustrated in Fig. 2.



142
143 **Figure 2** Workflow of generating tree cover products for 2016-2021, including imagery preprocessing,
144 generation of tree cover map product, and accuracy validation.

145
146 **2.3.1 Definition of mapped tree cover**

147 Traditionally, forests are considered to meet specific criteria (tree cover and height). The Food and Agriculture
148 Organization (FAO) of the United Nations defines forests as land spanning more than 0.5 hectares with trees
149 higher than 5 m and a canopy cover above 10% (FAO, 2020). According to the United Nations Framework
150 Convention on Climate Change (UNFCCC), forests are defined as areas with a minimum canopy cover of
151 10-30%, minimum tree height of 2-5 m, and a minimum area of 0.1 ha (Parker et al., 2008).

152

153 In this study, tree cover is defined as any geographic area dominated by trees without a percentage of tree
154 coverage at the pixel level (Zanaga et al., 2020; Hansen et al., 2013). This is attributed to the fact that the
155 resolution of the Planet pixel (4.77 m) is closer to the size of trees in tropical areas. Next, we utilized Planet-
156 NICFI imagery to generate only a prototype tree cover map with a resolution of 4.77 m and trees higher than
157 5 m. Our tree cover map product serves as baseline data for forest cover analysis. Upon further development
158 of the map to include trees higher than 5/2-5 m, it can be utilized for deriving forest maps for various functions,
159 such as those provided by FAO and UNFCCC.

160

161 2.3.2 Preprocessing of imagery

162 We utilized the GEE platform to preprocess Planet-NICFI imagery and Sentinel-1 SAR data for generating
163 tree cover maps for the years 2016-2021 (Fig. 2). Specifically, following the methodology of Yang et al.
164 (2023), we first employed the `ee.ImageCollection.mosaic()` function to merge and assemble overlapping
165 Sentinel-1 SAR data over the specified time period into a seamless, continuous imagery. Subsequently, we
166 performed bilinear resampling on the SAR imagery, specifically the VV and VH bands, to match the spatial
167 resolution of Planet-NICFI imagery with a spatial resolution of 4.77 m.

168

169 Planet-NICFI offers imagery at two different temporal frequencies spanning from 2016 to 2021. This includes
170 semi-annual imagery from 2016 to 2019 and monthly data from 2020 to 2021. To create a coherent and
171 consistent dataset for 2020 and 2021, we synthesized the selected time window of monthly imagery into
172 single imagery for each band, namely red, green, blue, and near-infrared bands. Specifically, we utilized the
173 `ee.ImageCollection.min()` function on each monthly imagery to extract the minimum monthly imagery, which

174 was then used to generate the second semi-annual imagery for 2020 and 2021. This approach was employed
175 to minimize the impact of cloud pollution on Planet-NICFI imagery (Oishi et al, 2018).

176

177 2.3.3 Generation of time-series tree cover map product

178 In addition to applying the RF approach in our tree cover mapping (Yang et al., 2023), RF-based methods
179 have been widely employed to develop global LCLUC products and show good performance (Zanaga et al.,
180 2022; Zanaga et al., 2021; Buchhorn et al., 2020). To acquire the time-series tree cover map dataset, our
181 methodology involved a two-step process. Initially, we integrated our custom RF approach, implemented on
182 Google Earth Engine (GEE), with a cloud-based machine learning platform. This combination enabled us to
183 obtain semi-annual Planet-NICFI and Sentinel-1 imageries spanning the years 2016 to 2021, as illustrated in
184 Fig. 2. Following data acquisition, we performed several post-processing steps to generate accurate tree cover
185 map product for the SEA region. These steps included downloading the acquired data from the cloud platform
186 to a local location, conducting mosaic operations, clipping relevant areas, applying projection transformations,
187 and performing correlation statistics. By employing this comprehensive approach, we successfully produced
188 a high-resolution tree cover map product.

189

190 2.3.4 Statistical accuracy assessment

191 We used two methods to assess the statistical accuracy of our tree cover map product. The generated tree
192 cover map product is compared pixel by pixel with the tree cover/non-tree cover labels. We then obtained a
193 confusion matrix, including true tree cover (TP), true non-tree cover (TN), false tree cover (FP), and false
194 non-tree cover (FN). These four values are used to calculate the user's accuracy, producer's accuracy, and
195 overall accuracy at a 95% confidence level (Olofsson et al., 2014) and the F1 score based on Eqs. (1)-(4),
196 respectively.

$$\text{User's accuracy (UA)} = \frac{TP}{TP + FP} \quad (1)$$

$$\text{Producer's accuracy (PA)} = \frac{TP}{TP + FN} \quad (2)$$

$$\text{Overall accuracy} = \frac{TP + TN}{TP + TN + FP + FN} \quad (3)$$

$$\text{F1 score} = \frac{2 \times UA \times PA}{UA + PA} \quad (4)$$

197 In addition, following Tsendbazar et al. (2021), we used a stability index based on the user's and producer's
 198 accuracy to evaluate the time-series accuracy consistency of the tree cover map product. The stability index
 199 used to evaluate tree cover accuracy is expressed as

$$SI_{t1} = \frac{|TC_{t1} - TC_{t1-1}|}{TC_{t1-1}} \times 100 \quad (5)$$

200 where SI_{t1} is the stability index that indicates the accuracy of tree cover maps (user's or producer's accuracy)
 201 at time $t1$, TC_{t1} is tree cover accuracy at time $t1$ and TC_{t1-1} is tree cover accuracy at the previous time ($t0$
 202 or the reference year). We also used the maximum and average stability index for two consecutive years to
 203 assess the stability of our tree cover products over a long period.

204

205 **3 Results**

206 We employed two approaches to assess the performance of our Planet-NICFI 2016-2021 tree cover map
 207 product. Firstly, we estimated the accuracy of our tree cover products for each year to gain insights into their
 208 accuracy and consistency, based on the methods developed by Tsendbazar et al. (2021). In addition, we
 209 showed example time series tree cover maps and reported the area dynamics change of tree cover maps during
 210 2016-2021. Secondly, we compared our tree cover products to widely used global tree cover products at 10
 211 m resolution, including FROM-GLC10 in 2017 (Gong et al., 2019), as well as ESA WorldCover 2020 and
 212 2021 (Zanaga et al., 2022; Zanaga et al., 2021).

213

214 **3.1 Assessment of tree cover map product**

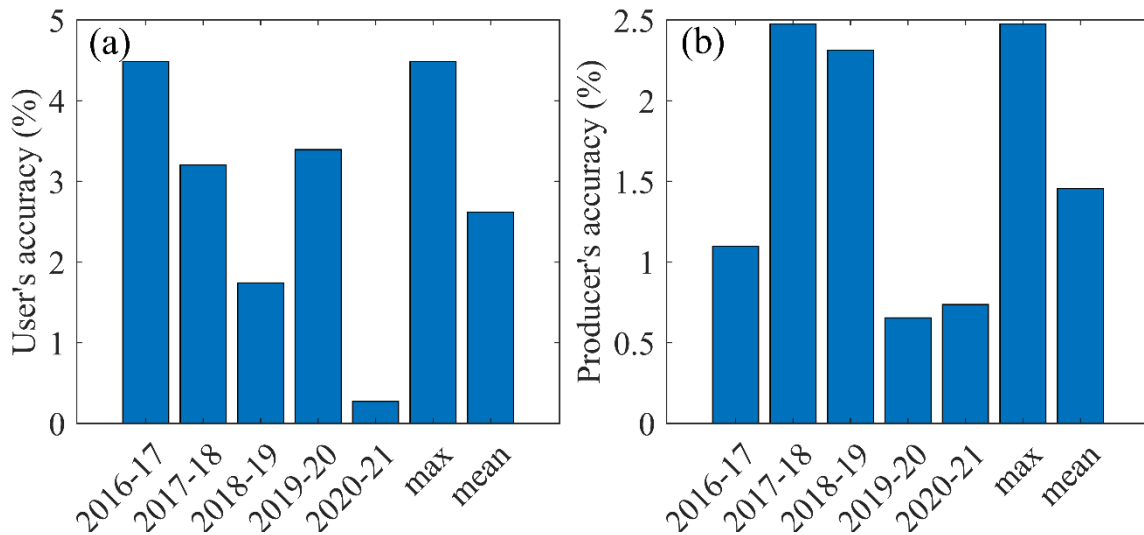
215 We reported the annual accuracy of the time-series Planet-NICFI tree cover map product in Table 2 with a
 216 95% confidence level. The tree cover accuracy results for 2019 were provided by Yang et al. (2023). The
 217 overall accuracy of the tree cover map product ranged between 0.867-0.907 ± 0.015 from 2016 to 2021, with
 218 the highest accuracy of 0.907±0.014 in 2021 and the lowest accuracy of 0.867±0.017 in 2016 (Table 2). This
 219 discrepancy could be due to poor data in the Planet-NICFI imagery during 2016. The F1 score showed a
 220 similar trend from 2016 to 2021, with an average of approximately 0.921. The user's accuracy consistently
 221 exceeded 0.901±0.017 over the six years, except for 2016 when it was 0.862±0.021. The producer's
 222 accuracies were all higher than 0.912±0.014 (Table 2). Nevertheless, the mapping results of our time-series
 223 Planet-NICFI tree cover maps were highly consistent. Additionally, compared to the tree cover, the non-tree
 224 cover showed lower user's accuracy, producer's accuracy, and F1 score (i.e., approximately 0.856±0.027,
 225 0.852±0.025, and 0.853, respectively), likely due to the complex composition of non-tree cover types, such
 226 as shrubland and herbaceous wetland.

227
 228 **Table 2** User's accuracies, producer's accuracies, F1 score, and overall accuracies of the Planet-NICFI V1.0
 229 2016-2021 tree cover map product for SEA at a 95% confidence level. The accuracy evaluation results in
 230 2019 were provided by Yang et al. (2023).

Year	Classification	User's accuracy	Producer's accuracy	F1 score	Overall accuracy
2016	Tree cover	0.862±0.021	0.925±0.018	0.892	0.867±0.017
	Non-tree cover	0.876±0.031	0.783±0.026	0.827	
2017	Tree cover	0.901±0.017	0.935±0.016	0.917	0.892±0.016
	Non-tree cover	0.874±0.033	0.814±0.027	0.843	
2018	Tree cover	0.929±0.016	0.912±0.014	0.920	0.892±0.015
	Non-tree cover	0.816±0.033	0.85±0.030	0.832	
2019	Tree cover	0.913±0.012	0.933±0.010	0.923	0.895±0.011
	Non-tree cover	0.857±0.022	0.819±0.021	0.837	
2020	Tree cover	0.944±0.014	0.927±0.011	0.935	0.900±0.014
	Non-tree cover	0.754±0.041	0.803±0.040	0.778	
2021	Tree cover	0.947±0.014	0.934±0.011	0.940	0.907±0.014
	Non-tree cover	0.778±0.038	0.816±0.039	0.796	

231

232 We also estimated the stability of our Planet-NICFI tree cover maps accuracy over 2016-2021 (Fig. 3). The
233 results show that the user's and producer's stability indexes were low than 4.5% and 2.5%, respectively,
234 indicating the good stability of our mapped Planet-NICFI tree cover maps for the six years (2016-2021).

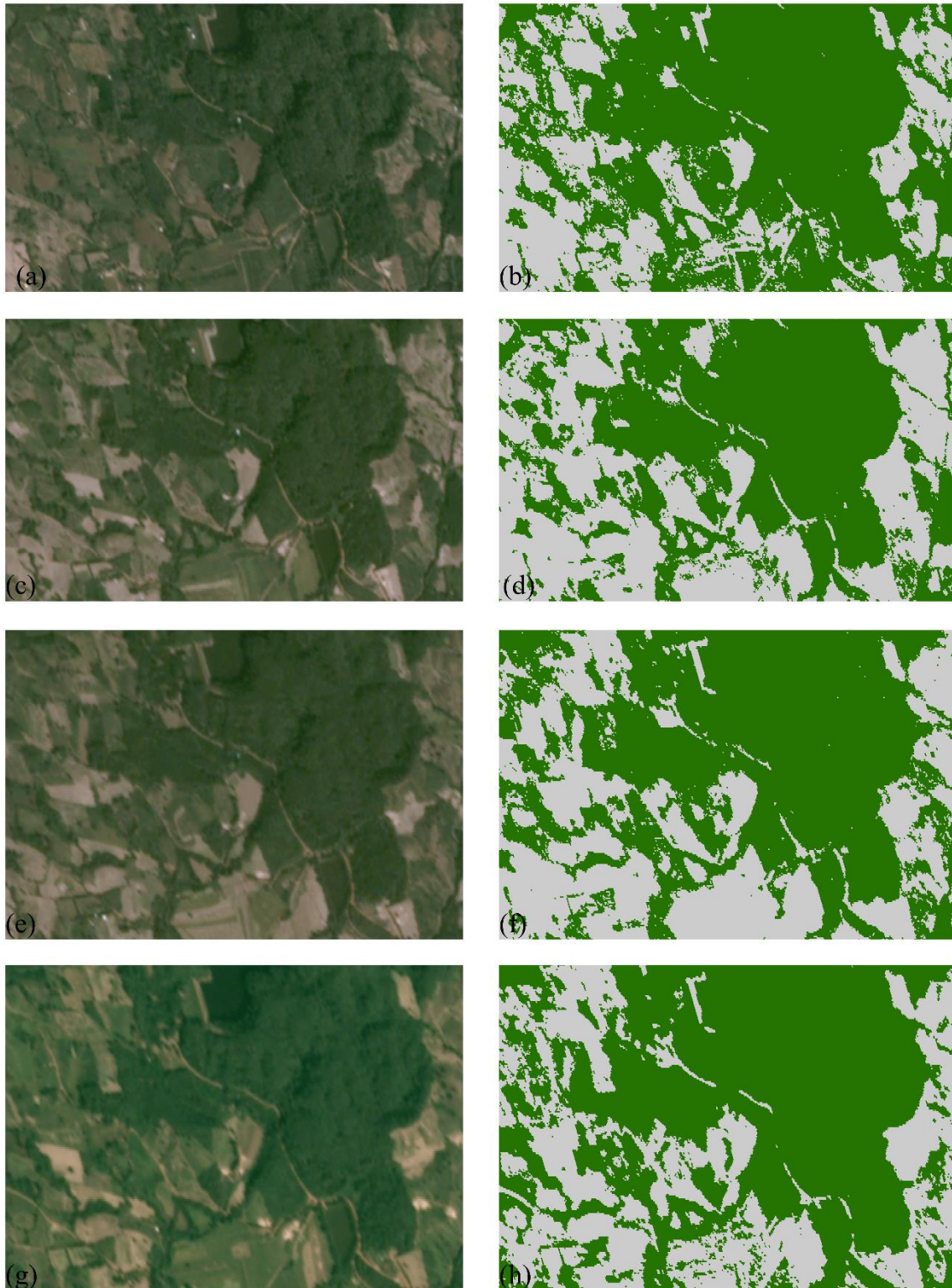


235 **Figure 3** Stability index estimates for the Planet-NICFI tree cover map product 2016-2021: the stability index
236 for (a) the user's accuracy and (b) the producer's accuracy.
237

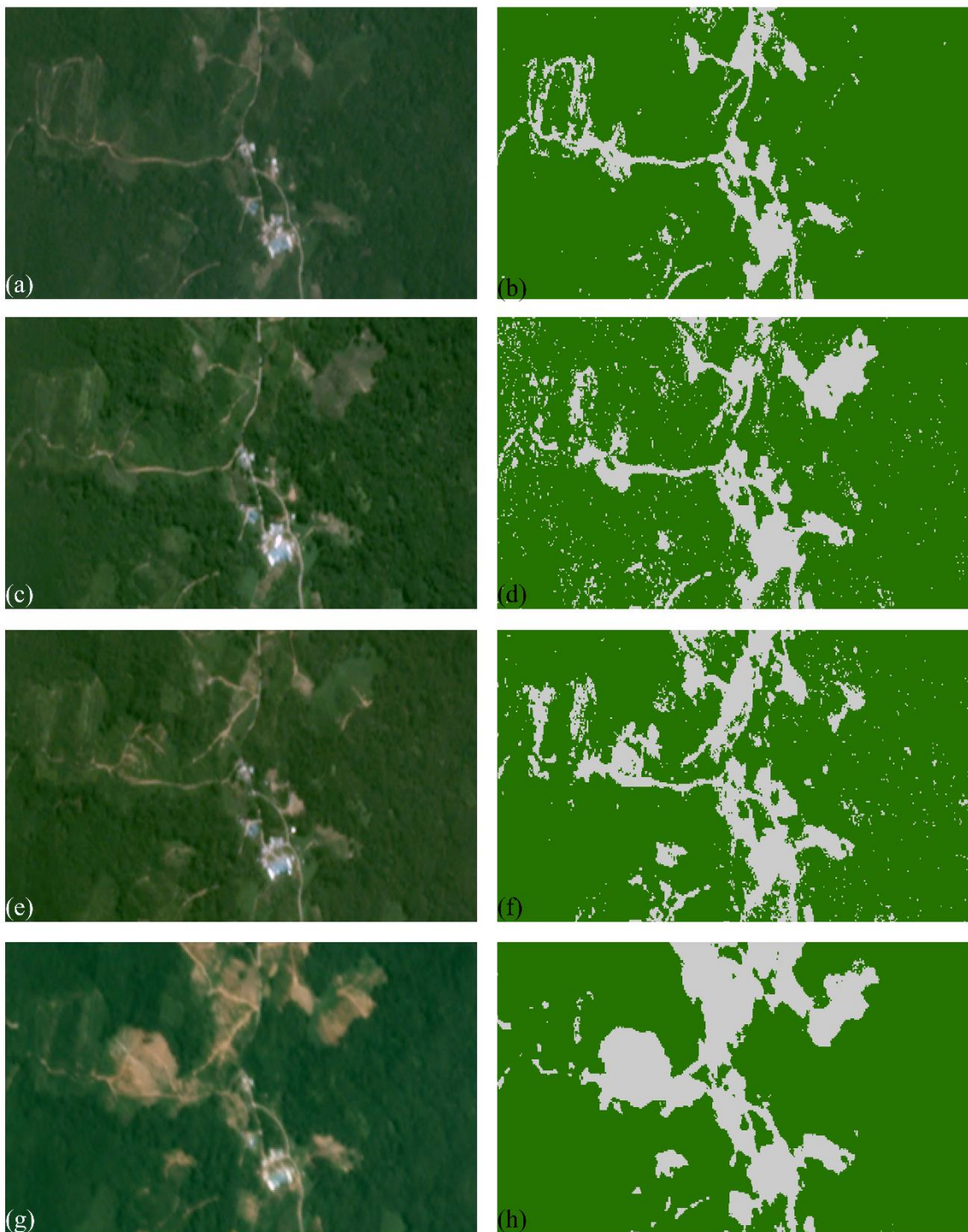
238

239 We further visually compared our time-series tree cover map product with the original Planet-NICFI imagery
240 during 2016-2019 (Figures 4-5). Note that we have not shown the years 2020 and 2021 due to inconvenient
241 visualization for monthly resolution Planet-NICFI imagery collected from QGIS. In comparison, our tree
242 cover map product showed better consistencies with Planet-NICFI imagery, such as roads, the spatial
243 distribution pattern of tree cover, and non-tree cover. However, our tree cover product potentially exhibited
244 salt and pepper salt and pepper phenomenon in some years (i.e., 2017 and 2018) due to the employment of
245 the RF approach. In practical applications, we need to pay attention to this phenomenon. In addition, we
246 counted the time series of the area estimates of tree cover maps during 2016-2021 and showed a slight
247 increase trend from 2016 to 2021, which is in line with the area estimates of ESA tree cover for the years
248 2020 and 2021. This may be due to forest restoration after the 2015 El Niño phenomenon (Wigneron et al.,

249 2020), as well as the impact of expanded plantations (Xu et al., 2020).



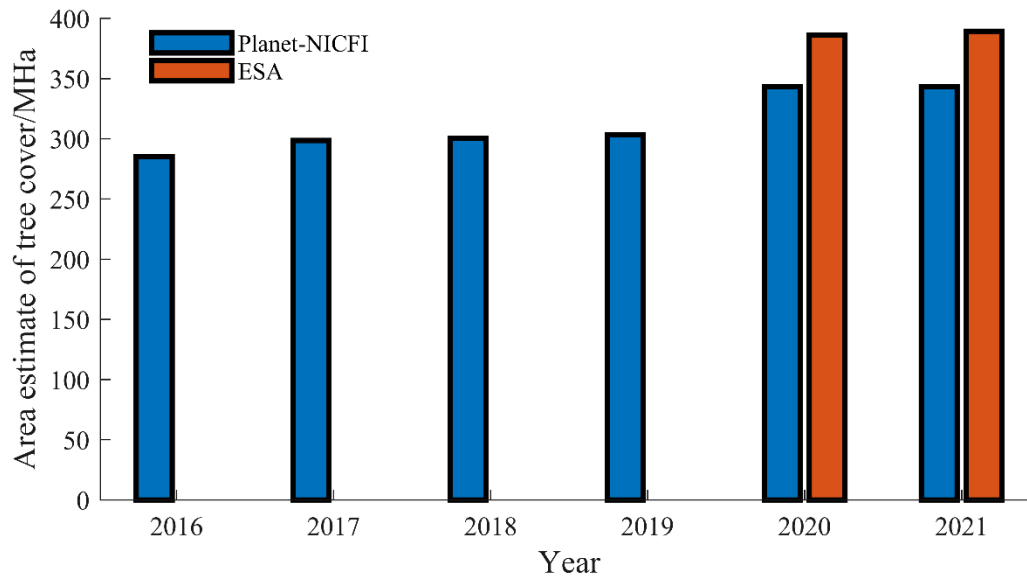
250
251 **Figure 4** Time series of the derived tree cover maps for the selected mainland SEA area (100.301°-100.322°E,
252 18.400°-18.409°N). (a) and (b), (c) and (d), (e) and (f), and (g) and (h) indicate 2019, 2018, 2017, and 2017,
253 respectively.



254

255 **Figure 5** Time series of the derived tree cover maps for the selected maritime SEA area (111.789°-111.806°E,
 256 2.032°-2.040°N). (a) and (b), (c) and (d), (e) and (f), and (g) and (h) indicate 2019, 2018, 2017, and 2017,
 257 respectively.

258

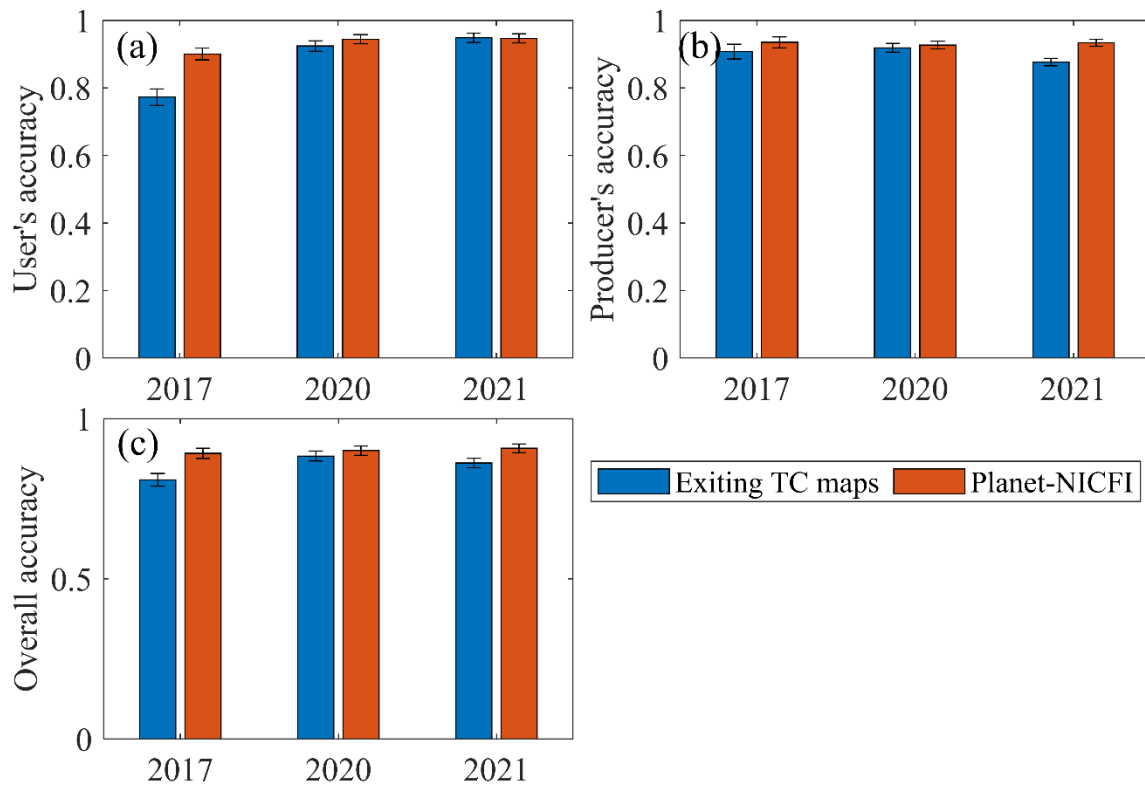


259
 260 **Figure 6** Area dynamics change of tree cover maps for Planet-NICFI and ESA from 2016 to 2021.

261

262 **3.2 Comparison with existing tree cover products**

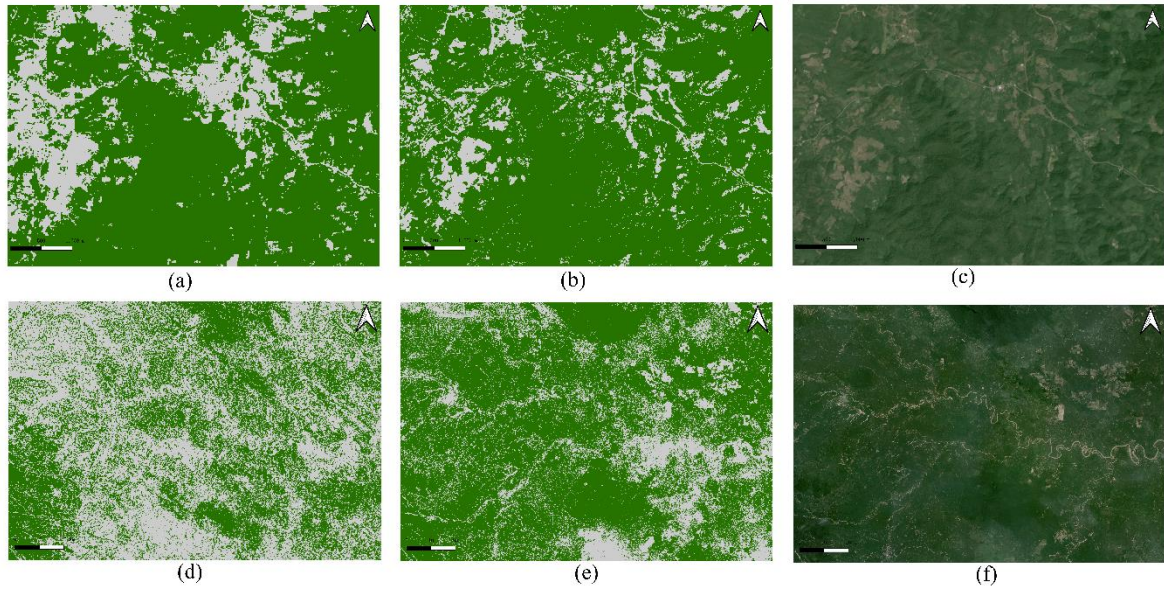
263 We compared our mapped Planet-NICFI tree cover maps with FROM-GLC10, ESA WorldCover 2020 and
 264 2021 regarding statistical accuracy (Fig. 4). The results show that our tree cover maps outperformed FROM-
 265 GLC10 in user’s accuracy, producer’s accuracy, and overall accuracy. The user’s accuracy and overall
 266 accuracy of our tree cover maps exceeded 0.083. ESA WorldCover 2020 and 2021 showed similar
 267 performances to our Planet-NICFI tree cover maps. Particularly, the user’s accuracy, producer’s accuracy,
 268 and overall accuracy of ESA WorldCover 2020 decreased by 0.020, 0.008, and 0.017, respectively (Fig. 4).
 269 This may be because we all used the SAR imagery as input and applied the RF-based machine learning
 270 method to classify our tree cover.



271
 272 **Figure 7** Accuracy comparison between existing tree cover maps and the generated Planet-NICFI tree cover
 273 maps at a 95% confidence level: (a) user's accuracy, (b) producer's accuracy, and (c) overall accuracy.

274

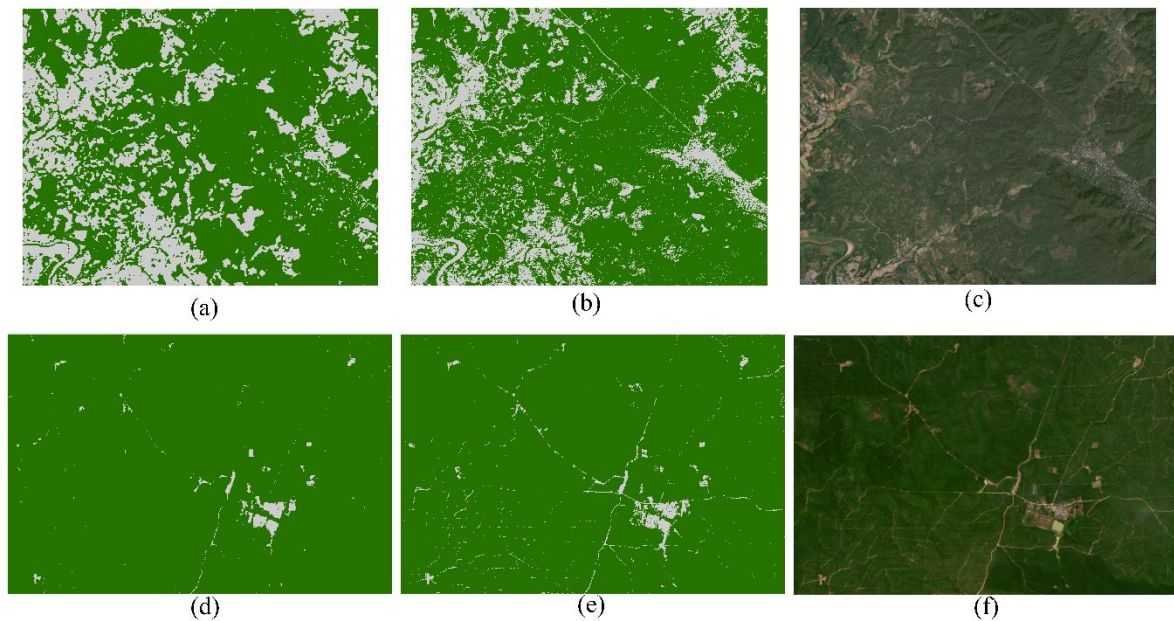
275 We selected six locations (three mainland SEA areas and three maritime SEA areas) to visually compare our
 276 Planet-NICFI tree cover maps with three other 10-meter products, namely, FROM-GLC10, ESA WorldCover
 277 2020 and 2021 (Figs. 8-10). In comparison, it is easier for FROM-GLC10 to classify all mixed tree and non-
 278 tree areas into non-tree cover maps (Fig. 8a). This may be because FROM-GLC10 cannot apply SAR imagery
 279 to tree cover mapping. However, ESA WorldCover 2020 and 2021 can capture tree cover landscapes at a
 280 higher level of detail than FROM-GLC, such as long narrow roads, croplands, and built-up areas (Figs. 9-
 281 10a). It should be noted that ESA WorldCover 2020 and 2021 omitted some long narrow non-tree cover
 282 landscapes and small isolated tree cover and non-tree cover landscapes due to the limitation of the imagery
 283 resolution (10 m).



284

285 **Figure 8** Comparison of FROM-GLC10 (a) and (d), Planet-NICFI tree cover (b) and (e), and Planet-NICFI
 286 imagery (c) and (f) for mainland SEA area (101.594°-101.651°E, 19.254°-19.294°N; top row) and maritime
 287 SEA area (101.925°-103.296°E, -2.096°-1.145°S; bottom row). Green and gray 20% indicate tree cover and
 288 non-tree cover, respectively.

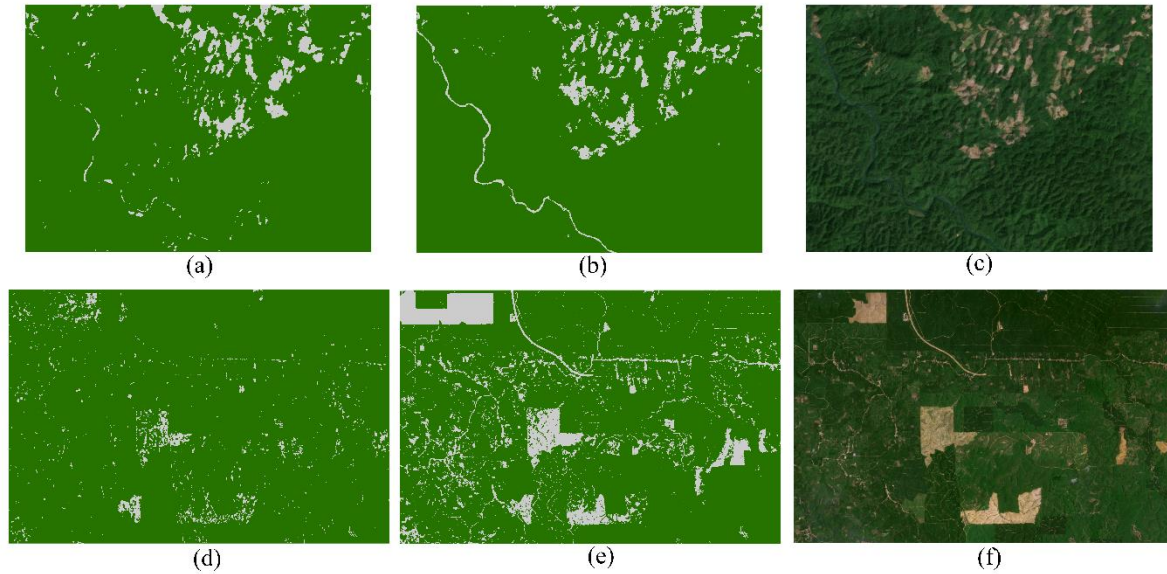
289



290

291 **Figure 9** Comparison of ESA WorldCover 2020 (a) and (d), Planet-NICFI tree cover (b) and (e), and Planet-
 292 NICFI imagery (c) and (f) for mainland SEA area (98.310°-98.392°E, 17.102°-17.166°N; top row) and
 293 maritime SEA area (99.983°-100.064°E, 1.387°-1.442°N; bottom row). Green and gray 20% indicate tree
 294 cover and non-tree cover, respectively.

295



296
 297 **Figure 10** Comparison of ESA WorldCover 2021 (a) and (d), Planet-NICFI tree cover (b) and (e), and Planet-
 298 NICFI imagery (c) and (f) for Mainland SEA area (102.179°-102.249°E, 18.676°-18.726°N; top row) and
 299 maritime SEA area (99.951°-100.063°E, 1.892°-1.967°E; bottom row). Green and gray 20% indicate tree
 300 cover and non-tree cover, respectively.

301

302 4 Discussion

303 Our time-series Planet-NICFI tree cover products were mapped twice a year to mitigate the impact of smog,
 304 light, cloud, and topographic effects in tropical areas (Roy et al., 2021; Marta et al., 2018). These high-
 305 resolution tree cover products meet the minimum tree height requirement of ≥ 5 m for further generating
 306 forest data. However, it should be noted that we cannot guarantee 100% tree cover for each higher-resolution
 307 pixel, which may introduce some uncertainties when using the higher-resolution tree cover maps. Despite
 308 excluding plantations during sample point labeling, some plantations, such as oil palm, may still be mixed
 309 into our tree cover products due to similarities in anomalies (Mugabowindekwe et al., 2023; Zanaga et al.,
 310 2022; Zanaga et al., 2021). As a result, caution should be exercised when using our Planet-NICFI tree cover
 311 products for certain purposes.

312

313 To generate a high-resolution time series tree cover map product at a continental scale, we utilized advanced

314 random forests-based machine learning algorithms on the GEE platform. However, for fine-scale tree cover
315 mapping, deep learning-based segmentation methods, such as U-net (Falk et al., 2019), are necessary,
316 particularly when using limited bands (Mugabowindekwe et al., 2023; Wagner et al., 2023; Zanaga et al.,
317 2022; Zanaga et al., 2021; Brandt et al., 2020). As a result, our tree cover map product still has some
318 uncertainty due to limitations in the optical PlanetScope imagery. To improve our tree cover mapping product
319 with higher resolution, we may need to consider adding more bands or utilizing advanced deep learning
320 algorithms in the future.

321

322 **5 Data availability**

323 The high-resolution Planet-NICFI V1.0 time-series tree cover product is now available at
324 <https://cstr.cn/31253.11.sciencedb.07173> (Yang and Zeng, 2023). This product is provided in the Mollweide
325 projection and the World Geodetic System 1984 (WGS1984) datum and geographic coordinate system. Tree
326 cover and non-tree cover are denoted as 0 and 1, respectively, in each yearly file, and are stored as UINT8 in
327 GeoTIFF format. The GeoTIFF files are named Planet-FC_SEA_<YEAR>_prj.tif, for example, Planet-
328 FC_SEA_16_prj.tif.

329

330 **6 Conclusions**

331 We have successfully generated the first accurate and high-resolution time-series tree cover map product for
332 SEA by combining optical and SAR satellite observations, utilizing advanced random forests machine
333 learning algorithms on the GEE platform. Our Planet-NICFI tree cover map product exhibits excellent
334 accuracy and consistency over six years (2016-2021). The baseline tree cover maps, with a resolution of 4.77
335 m, can be easily converted to forest cover maps at different resolutions to cater to the diverse needs of users.

336 Moreover, our tree cover map product has the unique ability to address rounding errors in forest cover
337 mapping by accurately capturing isolated trees and monitoring the removal of long, narrow forest cover.
338 These cutting-edge fine-scale time-series tree cover maps represent a milestone in forest monitoring and offer
339 unprecedented opportunities for users across diverse disciplines.

340

341 **Code Availability**

342 The scripts used to generate all Planet-NICFI v1.0 tree cover 2016-2021 are provided in JavaScript
343 (https://code.earthengine.google.com/?scriptPath=users%2Fyfhtaurus%2Fcodes%3APlanet_RF-LC_rac).

344 The maps can be automatically generated by running the codes. The scripts are also available on request from
345 Z. Zeng.

346

347 **Acknowledgments**

348 This study was supported by the National Natural Science Foundation of China (grant no. 42071022), the
349 start-up fund provided by the Southern University of Science and Technology (no. 29/Y01296122), and the
350 China Postdoctoral Science Foundation (grant no. 2022M711472). We thank Sen Jiang, Haowen Duan, Hao
351 Li, and Fangdong Fu for making tree cover/non-tree cover label data that are used to assess the time series
352 tree cover map products.

353

354 **Author contributions**

355 Z.Z. designed the research; F.Y. performed the analysis and wrote the draft. All authors contributed to the
356 interpretation of the results and the writing of the paper.

357

358 **Competing interests**

359 The authors declare no competing interests.

360 **References**

- 361 Achard, F., Beuchle, R., Mayaux, P. et al.: Determination of tropical deforestation rates and related carbon
362 losses from 1990 to 2010, *Glob Chang Biol*, 20(8), 2540-2554, 2014.
- 363 Brandt, M., Tucker, C. J., Kariryaa, A., et al.: An unexpectedly large count of trees in the West African Sahara
364 and Sahel, *Nature*, 587(7832), 78-82, 2020.
- 365 Buchhorn, M., Lesiv, M., Tsendbazar, N. E., et al.: Copernicus global land cover layers—collection 2, *Remote
366 Sens.*, 12(6), 1044, 2020.
- 367 Chen, J., Chen, J., Liao, A., et al.: Global land cover mapping at 30 m resolution: A POK-based operational
368 approach. *ISPRS J. Photogramm, Remote Sens.*, 103, 7-27, 2015.
- 369 CoP26, G. L.: Glasgow Leaders’ Declaration on Forests and Land Use. Available online at: [https://ukcop26.
370 org/glasgow-leaders-declaration-onforests-and-land-use/](https://ukcop26.org/glasgow-leaders-declaration-onforests-and-land-use/)(accessed December 06, 2021).
- 371 ESA: Land Cover CCI Product User Guide Version 2. Tech. Rep. Available at:
372 maps.elie.ucl.ac.be/CCI/viewer/download/ESACCI-LC-Ph2-PUGv2_2.0.pdf, 2017.
- 373 Falk, T., Mai, D., Bensch, R., et al. U-Net: deep learning for cell counting, detection, and morphometry, *Nat.
374 Methods*, 16(1), pp.67-70, 2019.
- 375 FAO: Global forest resources assessment 2020: Main report. Technical report, Food and Agriculture
376 Organization of the United Nations, ROME, 2020.
- 377 Friedl, M., Sulla-Menashe, D.: MCD12Q1 MODIS/Terra+Aqua Land Cover Type Yearly L3 Global 500m
378 SIN Grid V006. NASA EOSDIS Land Processes DAAC. Accessed 2022-12-15 from
379 <https://doi.org/10.5067/MODIS/MCD12Q1.006>, 2019.
- 380 Gong P., Liu H., Zhang M., et al.: Stable classification with limited sample: Transferring a 30-m resolution
381 sample set collected in 2015 to mapping 10-m resolution global land cover in 2017, *Sci. Bull*, 64, 370-
382 373, 2019.
- 383 Gorelick, N., Hancher, M., Dixon, M., et al.: Google Earth Engine: Planetary-scale geospatial analysis for
384 everyone, *Remote Sens. Environ.*, 202, 18-27, 2017.
- 385 Hammer, D., Kraft, R., Wheeler, D.: Alerts of forest disturbance from MODIS imagery, *Int J Appl Earth Obs
386 Geoinf*, 33, 1-9, 2014.
- 387 Hansen, M. C., Potapov, P. V., Moore, R., et al.: High-resolution global maps of 21st-century forest cover
388 change, *Science*, 342(6160), 850-853, 2013.
- 389 Hansen, M. C., Stehman, S. V., Potapov, P. V.: Quantification of global gross forest cover loss, *Proc Natl
390 Acad Sci USA*, 107(19), 8650-8655, 2010.
- 391 Hsieh, P. F., Lee, L. C., Chen, N. Y.: Effect of spatial resolution on classification errors of pure and mixed
392 pixels in remote sensing, *IEEE Trans. Geosci. Remote Sens.*, 39(12), 2657-2663, 2001.
- 393 Karra K., Kontgis C., Statman-Weil Z., et al.: Global land use/land cover with Sentinel 2 and deep learning.
394 In 2021 IEEE international geoscience and remote sensing symposium IGARSS (pp. 4704-4707), IEEE,
395 2021, July.
- 396 Lang, N., Jetz, W., Schindler, K. Wegner, J. D.: A high-resolution canopy height model of the Earth,
397 [doi:10.48550/arxiv.2204.08322](https://doi.org/10.48550/arxiv.2204.08322), 2022.
- 398 Marta, S.: Planet imagery product specifications, Planet Labs: San Francisco, CA, USA, 91, 2018.
- 399 Mugabowindekwe, M., Brandt, M., Chave, J., et al.: Nation-wide mapping of tree-level aboveground carbon
400 stocks in Rwanda, *Nat. Clim. Change*, 1-7, 2023.
- 401 Oishi, Y., Sawada, Y., Kamei, A., et al.: Impact of Changes in Minimum Reflectance on Cloud Discrimination,
402 *Remote Sens.*, 10(5), 693, 2018.

403 Olofsson, P., Foody, G.M., Herold, M., et al.: Good practices for estimating area and assessing accuracy of
404 land change, *Remote Sens. Environ.*, 148, 42-57, 2014.

405 Parker, C., Mitchell, A., Trivedi, M., Mardas, N.: The little REDD book: a guide to governmental and non-
406 governmental proposals for reducing emissions from deforestation and degradation. The little REDD
407 book: a guide to governmental and non-governmental proposals for reducing emissions from
408 deforestation and degradation,
409 http://www.globalcanopy.org/themedia/file/PDFs/LRB_lowres/lrb_en.pdf, 2008.

410 Planet Team: Planet Application Program Interface: In Space for Life on Earth. San Francisco, CA,
411 <https://api.planet.com>, 2017.

412 Reiner, F., Brandt, M., Tong, X., et al.: More than one quarter of Africa's tree cover found outside areas
413 previously classified as forest, 2022.

414 Roy, D.P., Huang, H., Houborg, R., Martins, V.S.: A global analysis of the temporal availability of
415 PlanetScope high spatial resolution multi-spectral imagery, *Remote Sens. Environ.*, 264, 112586, 2021.

416 Sexton, J.O., Noojipady, P., Song, X.P., Feng, M., Song, D.X., Kim, D.H., Anand, A., Huang, C., Channan,
417 S., Pimm, S.L., Townshend, J.R.: Conservation policy and the measurement of forests, *Nat. Clim.*
418 *Change*, 6(2), 192-196, 2016.

419 Shimada, M., Itoh, T., Motooka, T., Watanabe, M., Shiraishi, T., Thapa, R., & Lucas, R.: New global
420 forest/non-forest maps from ALOS PALSAR data (2007–2010), *Remote Sens. Environ.*, 155, 13-31,
421 2014.

422 Skea J., Shukla P. R., Reisinger A., et al.: Climate change 2022: Mitigation of climate change, IPCC Sixth
423 Assessment Report, 2022.

424 Tsendbazar, N., Herold, M., Li, L., et al.: Towards operational validation of annual global land cover maps,
425 *Remote Sens. Environ.*, 266, 112686, 2021.

426 Velasco, R.F., Lippe, M., Tamayo, F., et al.: Towards accurate mapping of forest in tropical landscapes: A
427 comparison of datasets on how forest transition matters, *Remote Sens. Environ.*, 274, 112997, 2022.

428 Wagner, F. H., Dalagnol, R., Silva-Junior, C. H., et al.: Mapping Tropical Forest Cover and Deforestation
429 with Planet NICFI Satellite Images and Deep Learning in Mato Grosso State (Brazil) from 2015 to 2021,
430 *Remote Sens.*, 15(2), 521, 2023.

431 Wigneron, J.P., Fan, L., Ciais, P., et al. Tropical forests did not recover from the strong 2015–2016 El Niño
432 event, *Sci. Adv.*, 6(6), p.eaay4603, 2020.

433 Xu, Y., Yu, L., Li, W., et al. Annual oil palm plantation maps in Malaysia and Indonesia from 2001 to 2016,
434 *Earth Syst. Sci. Data*, 12(2), pp.847-867, 2020.

435 Yang, F., Jiang X., Alan D. Ziegler, et al. Improved fine-scale tropical forest cover mapping for Southeast
436 Asia using Planet-NICFI and Sentinel-1 imagery, *J. Remote Sens.*, 2023.

437 Feng, Y., Ziegler, A. D., Elsen, P. R. et al.: Upward expansion and acceleration of forest clearance in the
438 mountains of Southeast Asia, *Nat. Sustain*, 4(10), 892-899, 2021.

439 Zanaga D., Van De Kerchove R., Daems D., et al.: ESA WorldCover 10 m 2021 v200,
440 <https://doi.org/10.5281/zenodo.7254221>, 2022.

441 Zanaga D., Van De Kerchove R., De Keersmaecker W., et al.: ESA WorldCover 10 m 2020 v100,
442 <https://doi.org/10.5281/zenodo.5571936>, 2021.

443 Zeng, Z., Estes, L., Ziegler, A. D., et al.: Highland cropland expansion and forest loss in Southeast Asia in
444 the twenty-first century, *Nat. Geosci*, 11(8), 556-562, 2018a.

445 Zeng, Z., Gower, D. and Wood, E. F.: Accelerating Forest loss in Southeast Asian Massif in the 21st century:
446 A case study in Nan Province, Thailand, *Glob Chang Biol*, 24, 4682-4695, 2018b.